Diffusion and nucleation of yttrium atoms on Si(111)7×7: A growth model

C. Polop,[1,2,*] E. Vasco,[1] J. A. Martín-Gago,[1] and J. L. Sacedón[1]
[1]*Instituto de Ciencia de Materiales de Madrid, CSIC, Cantoblanco, Spain 28049*
[2]*I. Physikalisches Institut, RWTH Aachen, 52056 Aachen, Germany*
(Received 8 February 2002; revised manuscript received 26 April 2002; published 23 August 2002)

The atomic diffusion of Y atoms on the Si(111)7×7 surface at room temperature is studied by using a combination of scanning tunneling microscopy and kinetic Monte Carlo simulations. The experiment provides the occupancy statistics of faulted and unfaulted half-cells by Y atoms. A model taking into account the attractive interactions among adsorbates which provides the best quantitative agreement with the experimental data by kinetic Monte Carlo simulations is introduced. For low Y coverages, single Y adatoms as well as clusters can be identified inside the 7×7 reconstruction half-cells in the scanning tunneling microscopy images. Single Y adatoms are highly mobile inside the halves, resulting in a characteristic fuzzy appearance of the half-cell. The Y adatoms as well as the clusters present strong electronic effects, which gives us information about their interaction with the substrate Si atoms.

DOI: 10.1103/PhysRevB.66.085324 PACS number(s): 68.43.Jk, 68.35.Ja, 81.05.Cy, 68.37.Ef

I. INTRODUCTION

The challenge that constitutes the understanding, at an atomic scale, of the physics mechanisms involved in the adsorption of metal atoms on semiconductor surfaces has been the object of numerous works. In contrast to metals, semiconductor materials usually present a highly corrugate potential energy surface for diffusing atoms due to the presence of localized electronic states. In particular, the Si(111)7×7 reconstruction, formed by large triangular half-unit cells of two different types (faulted *F* and unfaulted *U*), plays a crucial role during the first stages of nucleation on this substrate. A lot of work has been devoted to the study of adsorption and diffusion of different metal atoms (e.g., Pd, Ag, Pb, Tl, Au, Y, and Sn) on the 7×7 silicon surface constituting itself as a model system.[1–10]

The 7×7 reconstructed Si(111) surface is characterized by high energy barriers at the borders of the half-cells of the reconstruction for thermal diffusion of metal adsorbates.[11,12] Nevertheless, in spite of the slow diffusion that these high-energy barriers should produce at room temperature (RT) a tendency of the deposited metal atoms to aggregate inside the half-cells with stronger or weaker preference for occupied *F* half-cells has been established. In particular, there is experimental evidence in at least two cases of metal adsorbates, namely, Pb and Sn atoms, in which the mobile species diffuse preferably toward occupied first-neighboring half-cells.[3,10] In these inspected systems, it is experimentally observed that atoms adsorbed individually inside a half-cell (monomers) constitute unique mobile species at RT. In the case of Pb atoms,[3] the authors showed in consecutive scanning tunneling microscopy (STM) images, extracted from a movie, how a monomer jumps faster toward neighboring half-cells occupied by other atoms than toward empty half-cells. The authors concluded that Pb atoms on neighboring halves show a strong tendency to agglomerate, and thus some kind of long-range attractive interaction exists among adatoms. A similar behavior was observed for Sn atom adsorption.[10] In this case, the authors reported that Sn monomers jump at RT only to occupied neighboring half-cells, and no hops of Sn monomers were detected to free neighboring halves in spite of long periods of observations time (2–3 h).

The work which is reported in this paper was undertaken to obtain an insight into the kinetic mechanisms that determinate metal diffusion on the Si(111)7×7 surface. The yttrium was chosen for this purpose due to its negligible solubility in Si at RT.[13] Previous works focused on analyses of high-coverage phases obtained on annealed samples,[14–16] while less attention was paid to the initial stages of Y chemisorption at RT.[9,17] In this work, we systematically study Y atom adsorption on a 7×7 silicon surface at RT. A detailed STM analysis is presented in Sec. III. We identify two types of features in the STM images that have been associated to monomers and *clusters* (more than one Y atom inside a half-cell). At low coverages, the Y adatom nucleation has a similar behavior to that of other metallic atoms, i.e., it presents preferential adsorption at the *F* halves and a tendency toward aggregation inside the halves of the 7×7 silicon surface. Similar to those previously reported systems, experiments suggest the presence of attractive long-range interactions among adatoms.

As a further step toward the understanding of the diffusion and nucleation mechanisms of metallic adatoms on the 7×7 reconstruction, we introduce a model based on kinetic Monte Carlo (kMC) simulations which help us to understand the experimental data. The details of the model are described in Sec. IV. It will be shown that we obtain the best interpretation of the experimental results by introducing an attractive interaction among adatoms adsorbed on neighboring halves, as the experimental observations suggest. The good agreement found between the experimental data and the results from the calculations demonstrates the crucial role played by the long-range interactions between adsorbates in the interpretation of the results. Since our results fairly reproduces features common to the behavior of several studied metallic atoms deposited on Si(111)7×7, the proposed model can be generalized to other similar systems. The physical origin of the attraction among adatoms, which promotes the cluster formation, and the role or any mediation played by

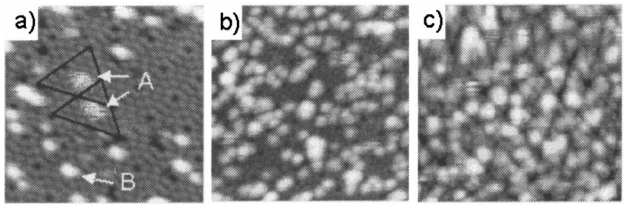

FIG. 1. Series of STM images of the Si(111)7×7 surface for increasing Y coverages: (a) 0.03 ML, (b) 0.1 ML, and (c) 0.2 ML. The scanned area is 150×150 Å^2. The bias voltage and tunneling current are 2 V and 0.7 nA, respectively.

the substrate in this long-range interaction still remain unclear.

II. EXPERIMENTAL PROCEDURE

Experiments were carried out in an ultrahigh vacuum (UHV) chamber equipped with low energy electron diffraction apparatus and a commercial scanning tunneling microscope (Omicron). The base pressure of the chamber was 1×10^{-10} mbar. All the STM images were recorded in a constant-current mode (topographic mode), with the bias voltage applied to the sample. Images were taken at different bias voltage in order to discriminate between topographic and electronic features. After carefully degassing the substrates [*n*-type P-doped Si(111), resistivity 0.1 Ωcm] at 600 °C for several hours, clean reconstructed Si(111)7×7 surfaces were prepared by flashing at 1200 °C. The samples were then slowly cooled from 900 °C to RT at a rate of 15 °C/min. Series of samples with variable Y coverage (θ) were prepared by using an electronic bombardment evaporator previously calibrated with a quartz crystal microbalance. During the evaporation, the substrate was always held at RT and the residual pressure in the UHV chamber remained below 8×10^{-10} mbar. The coverages are refereed to one unreconstructed Si(111) surface layer (1 ML=7.83×10^{14} atoms/cm^2) and were varied from 0.005–0.25 ML. The evaporation rate was 0.005 ML/s.

III. EXPERIMENTAL RESULTS

The topographic STM images in Fig. 1 illustrate the formation of Y clusters on the Si(111)7×7 surface for increasing coverages at RT. The surface is randomly decorated by bright features, which are localized inside the halves of the 7×7 unit cells. At these coverages ($\theta<0.25$ ML) the dimers and corner holes of the 7×7 reconstruction remain unaltered and the protrusions do not coalesce to form extend islands. Two kinds of features related to Y adsorption on the Si(111)7×7 surface can be resolved. Some halves present a fuzzy or noisy aspect [labeled *A* in Fig. 1(a)]. Others show well-defined protrusions [labeled *B* in Fig. 1(a)]. By similarity to other systems [Pb/Si(111)7×7,[3] Ag/Si(111)7×7,[7] and Sn/Si(111)7×7, (Ref. 10)] one could tentatively ascribe the first kind of structure (*A* type) to the adsorption of one single Y adatom inside a half-cell. The noisy aspect of the half-cells containing an *A*-type protrusion would be the result of the fast movement of a single adatom among different possible

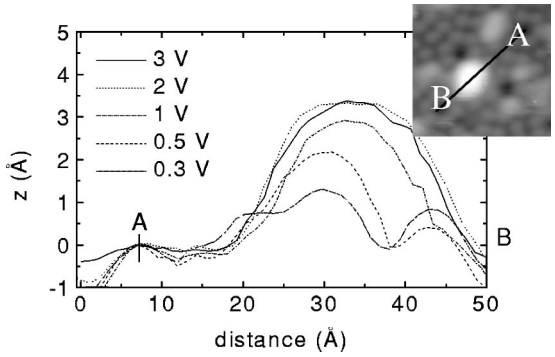

FIG. 2. Height profile across one *B*-type cluster from a series of topographic images at different voltages. The tunneling current is 0.7 nA.

adsorption sites inside the half-cell[11] at much faster rates than the STM scanning speed.

In addition, the image in Fig. 1(a) displays that the half-cells occupied by single atoms are surroundied by empty half-cells (in the image two triangles that confine the three neighboring halves of every monomer are drawn overimposed). After the evaluation of several experiments, we find that the latter condition is fulfilled by 91% of the monomers. This points out that, whenever an atom lands in a free half-cell with at least one occupied neighboring half-cell, it tends to diffuse toward this neighboring half-cell, thus only those monomers surrounding by empty half-cells present a high probability of remaining as individual atoms after the time of measurement. Thus experiments suggest the presence of an attractive interaction among adsorbates operating at long-range (intercell scale of nearest neighbors) similar to that previously reported for Pb/Si(111)7×7 and Sn/Si(111)7×7 systems.[3,10]

The second kind of protrusions (*B* type) presents some differences with respect to other reported systems (see, for instance Ref. 10). Probably due to its electronic configuration, the internal structure of the well-defined bright features (*B* type) cannot be clearly resolved. As shown in Fig. 2 the apparent high and profile of *B*-type protrusions changes strongly with the applied bias voltage. This fact hinders resolving the internal structure of the *B*-type features, and avoids a direct interpretation of the cluster structure from the STM data.

Two meaningful statistics values can be inferred from the STM images as a function of the coverage: the occupation *O* and the preference P_F for occupation of *F* half-cells. The occupation *O* is defined as the ratio of the number of half-cells occupied during the growth experiment to the number of half-cells on the surface, so that $0\leqslant O\leqslant1$. The preference P_F is determined as the ratio of the number of occupied *F* to the total number of occupied half-cells (by definition, $0\leqslant P_F\leqslant1$). Figures 3 (a) and (b) show the experimental dependence of *O* and P_F with the coverage (symbols). At a coverage as low as $\theta=0.03$ ML, the low obtained value of $O=0.28$ cannot be the result of a simple hit-and-stick growth mechanism (since this mechanism would imply that $O=0.52$). This result proves that during the deposition process and the time before the STM observations, some atomic re-

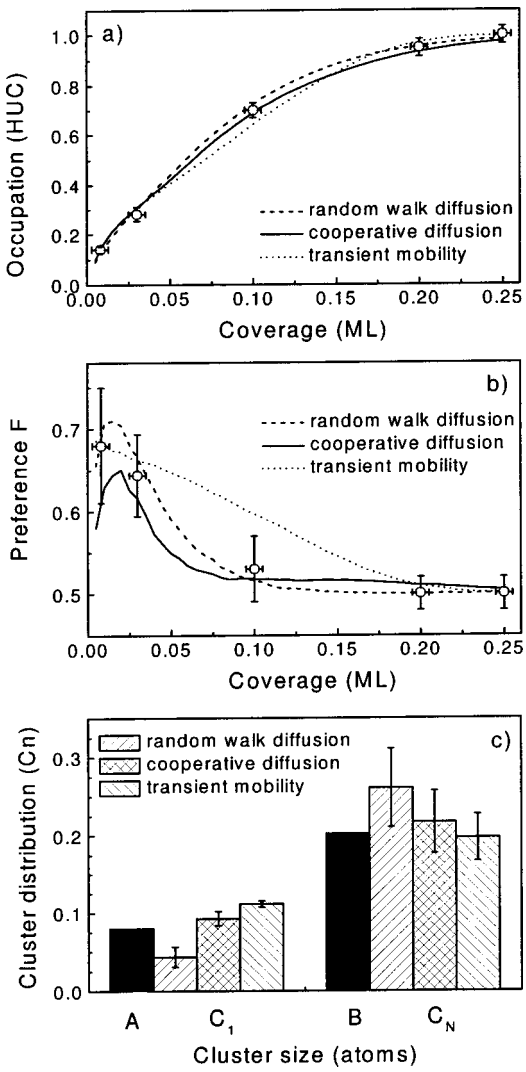

FIG. 3. (a), (b) The symbols correspond to the experimental occupation O and preference P_F as a function of the coverage. The lines correspond to the best fits found for the three different models described in the text. (c) The black bars correspond to the experimental concentrations of *A*- and *B*-type features for a coverage of $\theta=0.03$ ML. The pattern filled bars correspond to the C_1 and C_N theoretical concentrations for a coverage of $\theta=0.03$ ML for the three different models described in the text.

laxation mechanism that favors the agglomeration of adatoms takes place. At RT, when thermally activated hopping between half-cells seems to be negligible due to the high diffusion barrier that characterizes the semiconductor reconstructions, the origin of the agglomeration among adatoms into the half-cells could be given by two mechanisms previously suggested: a considerable reduction of the hopping barrier by the presence of adatoms in the nearest neighbor half-cells, due to a substrate-mediated long-range attractive interaction to favor the formation of clusters,[3] or the transient mobility of the adatom before it is nucleated on the Si(111)7×7 surface.[8]

As shown in Fig. 3(a), the occupation increases with the coverage until reaching the occupation of all the half-cells

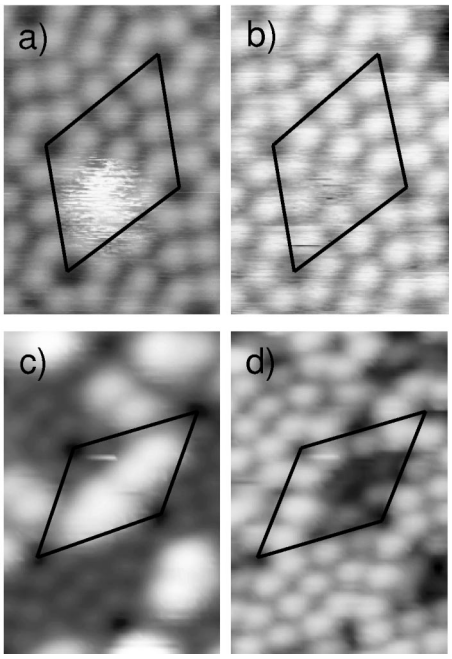

FIG. 4. STM images of the *A*-type [(a) and (b)] and *B*-type [(c) and (d)] features taken with a bias voltages of (a) 1.8 V, (b) 1.0 V, (c) 1.0 V, and (d) 0.3 V. A 7×7 reconstruction half-cell is drawn overimposed.

for $\theta=0.23$ ML. For higher coverages, further atoms start to be adsorbed on the dimer rows and corner holes of the 7×7 reconstruction.[9] This reveals that the half-cell has a limited capacity to accommodate atoms. 0.23 ML corresponds on average between five and six adatoms by a half-cell. In Fig. 3(b) we show the dependence of P_F as a function of the coverage. At coverages in the range of the thousands, P_F is around 0.7, which shows that the difference between F and U halves affects the growth. For higher coverages, P_F decreases until a saturation value 0.5, when all the half-cells are occupied. The tendency for the preferential adsorption on the F half-cell represents a general behavior for almost all metal atoms on this surface. Figure 3(c) shows the distribution of *A*- and *B*-type features on the surfaces for a coverage of $\theta=0.03$ ML (black bars). In the assumption that *A*-type features correspond to individual Y adatoms and *B*-type protrusions to clusters with several Y atoms, these values would correspond to the distribution of single adatoms (C_1) and clusters with n atoms ($C_N=\sum_n C_n$ with $n>1$) on the surface.

The electronic behavior of the fuzzy spots (A type) and the well-defined protrusions (B type) has been studied by STM. Both kinds of features are revealed as bright bumps for high bias voltages, as Figs. 4(a) and 4(c) show with high magnification. In Fig. 4(a) we show an overimposed 7×7 unit-cell which contains one *A*-type feature adsorbed on one half, while in Fig. 4(c) a 7×7 unit-cell which contains one B-type feature adsorbed on every half is overimposed. Figures 4(b) and 4(d) correspond to the same areas of Figs. 4(a) and 4(c), respectively, but measured at lower voltages. The corresponding 7×7 unit cells have been drawn overimposed. We observe that with the lowering of the bias voltage, the

apparent height of the bumps (both *A* and *B* types) diminishes until they disappear from the images, as the figure reveals. This effect is found for both polarities. The bias voltage at which clusters disappear from the STM images depends strongly on the cluster apparent size and also slightly on the tip condition[18].

The STM images taken at low bias voltage reveal a difference in the chemical interaction of the *A* and *B*-type features with the substrate Si atoms. In Fig. 4(b) it is observed that Si adatom dangling bonds of a half-cell occupied by an *A*-type feature appear unaltered in the image when lowering the bias voltage. This observation suggests that the adsorption of *A*-type features does not alter the distribution of the substrate density of states (DOS) on the half-cell. In contrast, by lowering the bias voltage on a half-cell occupied by a *B*-type feature, protrusions are replaced by dark spots in the images, as observed in Fig. 4(d). The latter observation suggests a modification of the substrate DOS, and thus of the Si, atom bondings, induced by the formation of *B*-type features. The changes in the images are reversible with the voltage and they are similarly observed for many different tips.

The fact that we obtain a tunneling current coming from the Y atoms only for high absolute values of the bias voltage can be understood in a first sight within the frame of the Thersoff-Hamman theory of STM (Ref. 19) as a semiconducting DOS for the adsorbed adatoms and clusters. However this interpretation could be very naive, and an accurate electronic description of the Y-Si bonding is required for a full understanding of the contrast change with the bias voltage in the STM images. The interesting issue to address here, related to the different diffusion behaviors of both kinds of observed features, is the nature of the bonds between Y adsorbed atoms and substrate Si atoms. A interpretation of the experimental observations will be addressed into the next sections.

IV. SIMULATION RESULTS

A deeper insight into the kinetics of adatom diffusion on Si(111)7×7 surface has been obtained with the help of kMC simulations. The simulations can be used to infer effective values of the parameters that play a major role on the adatom nucleation processes. The experiments (occupation *O* and preference P_F as function of the coverage, and cluster size distribution C_n for a given coverage) provide the information to determine these values. The potential energy surface of the 7×7 surface presents a high corrugation for the adatom diffusion due to the presence of localized electronic states with higher energy barriers at the borders of the triangular cells than between adsorption sites inside the half-cells. As a consequence, the diffusion on this surface is mainly driven by the energy barriers between neigboring halves, which provide the slowest jumping rates.

The simulation scheme used in this work, which is adopted from Ref. 20, uses the half-cell as a basic unit and ignores all processes that happen on smaller length scales (i.e., inside one half-cell). Therefore, the nucleation is modeled taking into account the diffusion process among adjacent halves, while the detailed description of adatom movement inside the half-cell is omitted. So, in the approximation of the potential energy surface with energy barriers only at the half-cell borders, every triangular cell is considered as one site of the lattice used to simulate the reconstructed surface. Note that in this intercell scale, the attractive contributions of the interatomic electrostatic potential predominates (for instance, taking into account the Morse or Lennard-Jones interatomic potential). In our model, any repulsive interatomic contribution that could operate at large scales[21] has been ignored, supported by the clear tendency of the adatoms to crowd inside the half-cells.

The surface is represented by a honeycomb lattice consisting of *F* and *U* sites representing the halves of the 7×7 reconstruction. Each site in the model is assigned two parameters: an indicator of the presence of a stacking fault (*F* or *U*), and the number of adatoms *n* inside the half-cell. The atoms arrive to the surface with a rate of $f=0.005$ ML/s, diffuse, and agglomerate on the Si(111)7×7 surface. Only hops of single adatoms through the dimer rows of the 7×7 reconstruction are allowed. Hops are considered to be thermally activated with a rate given by $\nu=\nu_0\exp(-E_{ij}/k_BT)$, where E_{ij} is the energy barrier to hop from site *i* to *j*, k_B is Boltzmann's constant, and *T* is the substrate temperature. The attempt frequency ν_0 is assumed to be the same for *F* and *U* halves. In the model, a critical cluster size i^* of the largest unstable Y cluster is used, and the half-cell capacity is limited to $n_{max}=5$ as the experimental data point out.

As evidenced by the experiments, metal atoms tend to agglomerate on this surface, not only due to the likely presence of attractive interactions among adsorbates in neighboring cells but also to the interaction with atoms adsorbed inside the same triangular cell. We do not analyze the internal structure of the clusters in detail but we assume that on average every Y atom interacts with the other Y atoms occupying the same half-cell by forming a number of Y-Y effective bonds defined as $(n-1)$. Note that the effective bonding energy used in this work (E_b) can be different from the covalent chemical bonding energy. Since every half-cell presents a lateral dimension of 26.8 Å, the distance between two atoms adsorbed into the same half-cell forming a *cluster* could be higher than the corresponding covalent bonding length. The maximum cluster size (maximum number of atoms inside a half-cell) sets the maximum number of Y-Y effective bonds to 4, and avoids high and unlikely values. Simulations were performed on a 150×150 half-cell lattice with periodic boundary conditions.

In order to compare the influence of the different mechanisms proposed in the literature on the nucleation of adatoms on the Si(111)7×7 surface, three different cases were tested. In the first case, we model random walk diffusion without the presence of long-range interaction between adatoms and/or clusters. In this case, the diffusion is isotropic, the energy barrier only depends on the state of site *i* and it is given by $E_{ij}=E_d^{F/U}+E_i=E_d^{F/U}+(n_i-1)E_b$. The first term of the expression corresponds to the surface contribution, different for *U* and *F* half-cells. We have simulated the preference for the adatoms to be adsorbed on the *F* half-cell of the reconstruction by considering a higher energy barrier to escape from *F* half-cells than from *U* half-cells ($E_d^F>E_d^U$).

TABLE I. Parameters used in the three models described in the text. (*) The maximum unstable cluster size of $i^*=1$ obtained for the random walk diffusion case makes the result of the model independent of the parameter E_b.

	Random diffusion	Cooperative diffusion	Transient mobility
ν_0 (s^{-1})	5×10^9	5×10^9	-
i^*	1	1	-
E_d^U (eV)	0.75	0.92	-
E_d^F (eV)	0.78	0.96	-
ΔE (eV)	0.03	0.04	0.02
E_b (eV)	- (*)	0.10	0.5
R	-	-	1

The second term of the expression for the energy barrier models the interaction between adatoms inside the same cluster as a linear function of the number (n_i-1) of Y-Y effective bonds that the adatom forms inside the *i* half-cell.

In the second case, we model the thermal diffusion with the reduction of the hopping barrier by the presence of adatoms in the nearest-neighboring half-cells, due to a long-range attractive intercell interaction which favors cluster formation. Therefore, the states of sites *i* and *j*, before and after the hop, must be considered. In *cooperative* diffusion, as we refer to this case hereafter, the surface migration is modeled as hopping process with an energy barrier given by $E_{ij}=E_d^{F/U}+(E_i-kE_j)=E_d^{F/U}+(n_i-1-kn_j)E_b$, where (n_i-1) and n_j are the number of Y-Y effective bonds in the cells formed by the adatom before and after a hop. *k* represents a spatial attenuation factor of the long-range interactions, which contains information about the interatomic attraction potential on the reconstructed Si(111)7×7 surface. In the extreme case where $k\to0$ the behavior of the *cooperative* diffusion tends to the random walk diffusion. For our simplified model, it has been chosen as $k=1$. Note that for the *cooperative* diffusion case, the height of the barrier depends on the jump direction and the diffusion is anisotropic.

The kinetic mechanism modeled in the third case is the transient mobility of the impinging adatoms before they are accommodated on the Si(111)7×7 surface. Landed adatoms statistically choose the energy minimum position inside an available area, which is defined by the incorporation radio *R* (where $R=q$ means area defined by the *q*th nearest neighboring halves). In this case, the energy of the adatom inside a half-cell is given by the expressions $E^F=\Delta E+nE_b$ and $E^U=nE_b$ for the *F* and *U* half-cells respectively, where $\Delta E=E^F-E^U$.

The lines in Figs. 3(a)–3(b) represent the best fits with the *O* and P_F experimental data achieved independently by the three models. In Fig. 3(c), the experimental *A*- and *B*-type feature concentrations are compared with the concentrations of single adatoms (C_1) and clusters (C_N) derived from every model (pattern filled bars). The best parameters calculated for each kMC-simulated case are summarized in Table I.

In Figs. 3(a)–3(b), we observed that the theoretical results from random walk diffusion model (dashed lines) show a good agreement with *O* and P_F experimental data. However, by the random walk diffusion model we can not adjust the distribution of *A*- and *B*-type features to that of clusters. For every set of parameters that gives a good agreement with the *O* and P_F experimental data, the calculated distribution of monomers is always 50% lower than the experimental distribution of *A*-type features, as observed in Fig. 3(c). In addition, this model omits the experimental evidence about the presence of long-range interactions between adsorbates exposed in Sec. III. All these reasons make us discard the random diffusion model to explain the experimental results presented in this work.

With the third simulated mechanism (i.e the transient mobility), we obtain a good agreement with the experimental *O* [dotted lines in Fig. 3(a)]. However, difficulties appear in obtaining a good agreement with the experimental P_F and the distribution of *A*-type features as monomers [see Figs. 3(b) and 3(c)]. The behavior of the P_F theoretical curve (constant negative slope) is clearly different to the experimental one. Theoretical and experimental works have shown that transient mobility of metal atoms on metal surfaces is a small effect. This is due to the low kinetic energy of the evaporated atoms (0.1 eV) and the effective dissipation process of the kinetic energy of adsorbates on metal surfaces.[22] Similarly, there is neither experimental nor theoretical evidence supporting the transient mobility mechanism of metal adsorbates on semiconductor surfaces. The transient mobility has only been shown in few systems such as Xe adsorption on Pt(111) surface or O adsorption on Al(111) surface.[23,24] In the latter case, the O transient mobility is only 5 Å on average.[24] Note that in our model every single jump corresponds to a length of 26.8 Å. Thus, contrary to what was proposed by Myslivecek *et al.*[8] for the adsorption of Ag atoms on the Si(111)7×7 surface, the abridgment of reasons exposed above again make us discard this model to explain our experimental data.

The cooperative diffusion model provides the best interpretation of all the experimental data: *O*, P_F and the distribution of *A*- and *B*-type clusters, as observed in Fig. 3. The simulation results fall within the error bars of the experimental data. In addition, this model explains the phenomenon of tendency to aggregation among adsorbates in neighboring half-cells. Both facts make us choose the *cooperative* diffusion as the correct model that explains the behavior of our experimental data.

V. DISCUSSION

The best quantitative agreement with the experimental data was obtained by taking into account the *cooperative* diffusion. The good agreement achieved by the assignation of the *A*- and *B*-type feature concentrations with the concentration of individual adatoms (C_1) and clusters (C_N) respectively, supports the interpretation of the fuzzy spots imaged in Fig. 1 as single adatoms (*A* type) and of the well-defined protrusions as clusters with several Y adatoms (*B* type).

The experimental value found for the attempt frequency, $\nu_0=5\times10^9$ s^{-1}, is orders of magnitude lower than the value of 10^{11}–10^{13} s^{-1} deduced for the adatoms diffusion on metal surfaces. Whereas each lattice site of the model corresponds

to a lateral length of 26.8 Å, a reinterpretation of the physical meaning of the attempt frequency on this model is needed. Similar values have also been obtained for the diffusion of Ag atoms on Si(111)7×7 system.[8] Taking into account that the *intracell* diffusion barriers are about 0.48 eV by using the hopping energy barrier for the three valence elements reported by Cho and Kaxiras,[11] the *intracell* hopping frequency of a single adatom can be estimated to be about 20 s^{-1} for $\nu_0 = 5 \times 10^9$ s^{-1}. This fact explains the fuzzy appearance of the single adatoms, considering that the average scanning frequency of one half-cell is 0.25 s^{-1}.

The maximum unstable cluster size derived from our model, $i^* = 1$, means that only Y single adatoms diffuse among neighboring half-cells on the Si(111)7×7 surface at RT. Our result agrees with previous STM observations about the diffusion of Pb and Sn adatoms on the Si(111)7×7 surface,[3,4,10] where at RT only jumps of single adatoms were observed between adjacent halves. It is interesting to note the high energy barrier $E_d = 0.92$ eV found in this work compared to the diffusion barriers of several metal surfaces for instance, $E_d = 0.26$ eV for Pt adatoms on Pt(111), $E_d = 0.35$ eV for Cu adatoms on Ni(001), or $E_d = 0.17$ eV for Ag adatoms on Pt(111) [Refs. 25–27]. However, the obtained energy barrier is similar to that obtained for diffusion of monomers across the dimer rows of the Si(001) surface ($E_d = 0.8$-1 eV).[28]

The slight difference among the substrate contributions for the two unequivalent halves of the 7×7 reconstruction ($\Delta E = 0.04$ eV) can be explained by their structural or electronic differences. The preferential adsorption on the *F* half-cell of the Si(111)7×7 has also been observed for others elements: 70% for Au atoms,[29] 80% for K atoms,[30] 89% for Li atoms,[31] 95% for Pd atoms,[1] nearly 90% for Ag atoms,[6] and 100% for Tl atoms.[5] Among the postulated arguments employed to explain the different adsorption probability between both halves, the different electronic structure of both is considered one of the main reasons.[12] The DOS of the adatoms of *F* is higher than in *U*, due to the structural differences produced by the stacking fault.[32] This produces a nonuniform distribution of charge on the 7×7 reconstruction and, likely, slight differences in the potential energy surface.

The STM images taken at low bias voltage reveal a difference in the interaction of the fuzzy spots, which have been ascribed to mobile monomers, and the well-defined protrusions, connected to stable clusters, with the substrate Si atoms. The adsorption of one single atom inside one half-cell does not alter the DOS of the substrate, pointing to a weak chemical interaction between the Y monomer and the substrate Si atoms. In contrast, the adsorption of two or more atoms inside one half-cell modified the DOS of the substrate pointing to a stronger bonding between the Y atoms forming the cluster and the Si atoms of the substrate. Stronger bonds normally correlate with larger diffusion energy barriers, which induces different kinetic behaviors for monomers and clusters. Only single atoms, which are weakly bonded to the subtrate and free of interactions with other intracell adsorbates, diffuse at RT fast between different adsorption sites inside the half-cell and at a lower frequency between adjacent halves. This experimental observation reinforces our calculation results.

The results presented here point to the significant role of long-range attractive interactions among adatoms in the diffusion of metal atoms on the Si(111)7×7 surface. The nature of the long-range interactions was recently investigated theoretically by density functional calculations and Monte Carlo simulations and experimentally by STM measurements in some metallic homoepitaxial system such as Al/Al(111) and Cu/Cu(111).[21,33,34] These studies revealed the importance of oscillatory long-range electronic interactions among adatoms on metal with a partial filled surface band such as in the Cu/Cu(111) system.[33,34] These indirect interactions are substrate mediated through the scattering of surface electrons, which form a two-dimensional nearly free-electron gas on the substrate surface. The surface electron scattering by the adatoms generates standing wave patterns in the electron density that give rise to the interactions between scatterers. Repulsive long-range elastic interactions that arise from adsorbate and substrate relaxations mediated via the atomic lattice are present in the Al/Al(111) system.[33]

In contrast, there is very little information about the long-range interactions between adatoms adsorbed on semiconductor surfaces, and in particular, about the nature of substrate-mediated interactions. The electronic mechanism for metals described above is not appropriate for semiconductor surfaces. In the case of a Si(111)7×7 reconstruction, a partially filled surface band that appears due to the arrangement of the dangling bonds provides metal-like features to the reconstructed surface. Although these states are close to the Fermi level they are localized and so far, there is no experimental evidence supporting that these states could become involved in the long-range interaction between adsorbed adatoms. However, this work provides evidence about the existence of an attractive interaction among metal adatoms contributing to reduce the hopping energy barriers between adjacent half-unit cells of the 7×7 reconstruction. Therefore, another different mechanism should be connected with this experimental fact, and likely it would be a combination of different processes. Electrostatic long-range interaction could be a possible explanation. Adatoms can sense each other through direct Coulomb interactions between the various multipoles that arise due to surface-induced charge redistribution on the adsorbates, although these interaction are typically relatively weak. A definitive and complete picture of the nature and characteristics of long-range adatom-adatom interactions on semiconductor surfaces and their correlation with the surface electronic structure can only come from further investigations.

VI. CONCLUSIONS

Due to the high diffusion barriers present on the dimer rows and corner holes of the Si(111)7×7 surface, a long-range attractive interaction among single adatoms and between single adatoms and clusters is necessary to explain the STM results about the dependence of the density of clusters, the *F* adsorption preference, and the cluster distribution on

the coverage. This interaction favors a *cooperative* diffusion mechanism that accounts for a reduction of the hopping energy barriers. The combined study of STM and kMC simulations reveals that only highly mobile Y single adatoms, almost trapped inside the half-cell, perform jumps between different halves at RT; therefore, the cluster size evolution depends only on the monomer aggregation rate.

ACKNOWLEDGMENTS

We acknowledge Gómez-Rodríguez for useful conversations and for a valuable critique of the manuscript's first draft, and to T. Michely for critical comments. This work was supported by Spanish National Project No. PB98-0524 and the regional CAM project 07N/0028/1999.

*Email address: polop@physik.rwth-aachen.de

[1] U.K. Köhler, J.E. Demuth, and R.J. Hamers, Phys. Rev. Lett. **60**, 2499 (1988).
[2] S. Tosch and H. Neddermeyer, Phys. Rev. Lett. **61**, 349 (1988).
[3] J.M. Gómez-Rodríguez, J.J. Sáenz, A.M. Baró, J.Y. Veuillen, and R.C. Cinti, Phys. Rev. Lett. **76**, 799 (1996).
[4] J.Y. Veuillen, J.M. Gómez-Rodríguez, A.M. Baró, and R.C. Cinti, Surf. Sci. **377**, 847 (1997).
[5] L. Vitali, M.G. Ramsey, and F.P. Netzer, Phys. Rev. Lett. **83**, 316 (1999).
[6] P. Sobotík, I. Ost'ádal, J. Myslivecek, and T. Jarolímek, Surf. Sci. **454-456**, 847 (2000).
[7] T. Jarolímek, J. Myslivecek, P. Sobotík, and I. Ost'ádal, Surf. Sci. **482-485**, 386 (2001).
[8] J. Mysliveček, P. Sobotík, I. Ošt'ádal, T. Jarolímek, and P. Šmilauer, Phys. Rev. B **63**, 045403 (2001).
[9] C. Polop, J.L. Sacedón, and J.A. Martín-Gago, Surf. Sci. **454-456**, 842 (2000).
[10] O. Custance, I. Brihuega, J.M. Gómez-Rodríguez, and A.M. Baró, Surf. Sci. **482-485**, 1406 (2001).
[11] K. Cho and E. Kaxiras, Surf. Sci. **396**, L261 (1998).
[12] Ph. Sonnet, L. Stauffer, and C. Minot, Surf. Sci. **407**, 121 (1998).
[13] Landolt-Börnstein Vol. III/22b, *Semiconductors: Impurities and Defects in Group IV Elements and II-V Compounds*, edited by M. Schulz, Landolt-Börnstein, New series Group II, Vol. 22, pt b (Springer-Verlang, Berlin, 1989).
[14] R. Baptist, S. Ferrer, G. Grenet, and H.C. Poon, Phys. Rev. Lett. **64**, 311 (1990).
[15] L. Magaud, A. Pasturel, G. Kresse, and J. Hafner, Phys. Rev. B **58**, 10 857 (1998).
[16] C. Polop, C. Rogero, J.L. Sacedón, and J.A. Martín-Gago, Surf. Sci. **482-485**, 1337 (2001).
[17] A. Pellissier, R. Baptist, and G. Chauvet, Surf. Sci. **210**, 99 (1989).
[18] Experimental observations pointed out a decrease of the bias voltage at which clusters disappear from the STM images as the apparent size of the cluster increases, indicating a metalization process induced by the increase of Y atoms in the cluster (Ref. 9). We have observed that the cluster of Fig. 2 disappears from the image at much lower voltage than the clusters of Figs. 4(c) and 4(d), probably due to the number of Y atoms forming every cluster, and also influenced by the tip conditions.
[19] J. Tersoff and D.R. Hamann, Phys. Rev. Lett. **50**, 1998 (1983).
[20] B. Voigtländer, M. Kästner, and P. Šmilauer, Phys. Rev. Lett. **81**, 858 (1998).
[21] K.A. Fichthorn and M. Scheffler, Phys. Rev. Lett. **84**, 5371 (2000).
[22] J.V. Barth, Surf. Sci. Rep. **40**, 1 (2000) and references therein.
[23] P.S. Weiss and D.M. Eigler, Phys. Rev. Lett. **69**, 2240 (1992).
[24] M. Schmid, G. Leonardelli, R. Tschelie β nig, A. Biedermann, P. Varga, Surf. Sci. **478**, L355 (2001).
[25] M. Bott, M. Hohage, M. Morgenstern, Th. Michely, and G. Comsa, Phys. Rev. Lett. **76**, 1304 (1996).
[26] B. Müller, L. Nedelmann, B. Fischer, H. Brune, and K. Kern, Phys. Rev. B **54**, 17 858 (1996).
[27] H. Brune, G.S. Bales, J. Jacobsen, C. Boragno, and K. Kern Phys. Rev. B **60**, 5991 (1999).
[28] J. Dabrowski and H-J. Müssig, *Silicon Surfaces and Formation of Interfaces* (World Scientific, Singapore, 2000).
[29] Ilya Chizhov, Geunseop Lee, and Roy F. Willis, Phys. Rev. B **56**, 12 316 (1997).
[30] A. Watanabe, M. Naitoh, and S. Nishigaki, Jpn. J. Appl. Phys. **37**, 3778 (1998).
[31] Y. Hasegawa, I. Kamiya, T. Hashizume, T. Sakurai, H. Tochihara, M. Kubota, and Y. Murata, J. Vac. Sci. Technol. A **8**, 238 (1990).
[32] L. Stauffer, S. Van, D. Bolmonnt, J.J. Koulmann, and C. Minot, Solid State Commun. **85**, 935 (1993).
[33] A. Bogicevic, S. Ovesson, P. Hyldgaard, B.I. Lundqvist, H. Brune, and D.R. Jennison, Phys. Rev. Lett. **85**, 1910 (2000).
[34] J. Repp, F. Moresco, G. Meyer, K.-H. Rieder, P. Hyldgaard, and M. Persson, Phys. Rev. Lett. **85**, 2981 (2000).